THE ASTROPHYSICAL JOURNAL, 555:925–931, 2001 July 10
© 2001. The American Astronomical Society. All rights reserved. Printed in U.S.A.

INFRARED SPACE OBSERVATORY SPECTRA OF R CORONAE BOREALIS STARS. I. EMISSION FEATURES IN THE INTERVAL 3–25 MICRONS[1]

DAVID L. LAMBERT
Department of Astronomy, University of Texas, Austin, TX 78712-1083; dll@astro.as.utexas.edu
N. KAMESWARA RAO
Indian Institute of Astrophysics, Koramangala, Bangalore 560034, India; nkrao@iiap.ernet.in
AND
GAJENDRA PANDEY AND INESE I. IVANS
Department of Astronomy, University of Texas, Austin, TX 78712-1083;
pandey@astro.as.utexas.edu, iivans@astro.as.utexas.edu
Received 2001 January 16; accepted 2001 March 16

ABSTRACT

Infrared Space Observatory 3–25 μm spectra of the R Coronae Borealis stars V854 Cen, R CrB, and RY Sgr are presented and discussed. Sharp emission features coincident in wavelength with the well-known unidentified emission features are present in the spectrum of V854 Cen but not in the spectra of R CrB and RY Sgr. Since V854 Cen is not particularly hydrogen-poor and has 1000 times more hydrogen than the other stars, the emission features are probably from a carrier containing hydrogen. There is a correspondence between the features and the emission from laboratory samples of hydrogenated amorphous carbon. A search for C_{60} in emission or absorption proved negative. Amorphous carbon particles account for the broad emission features seen between 6 and 14 μm in the spectrum of each star.

Subject headings: circumstellar matter — infrared: stars — stars: variables: other

1. INTRODUCTION

The rare class of peculiar stars known as the R Coronae Borealis (R CrB) stars possess two very distinctive characteristics: a propensity to fade at unpredictable times by up to about 8 mag and an F–G supergiant-like atmosphere that is very H-deficient and He-rich, and has considerable amounts of carbon. The fading of the visible light is often rapid, with deep minima achieved in a few days to a few weeks, but the return to maximum light is generally slower, occurring over a period of several months. O'Keefe's (1939) suggestion that an R CrB star fades when a cloud of soot forms to obscure the photosphere has stood the test of time, but the detailed identification of the dust particles and their mode and site of formation remain open questions.

Infrared photometry and low-resolution spectroscopy of R CrB stars at maximum light and in decline have revealed several key features of the dusty circumstellar shells. Discovery of infrared excesses provided confirmation of the hypothesis that dust grains were a major constituent of the circumstellar shells (Stein et al. 1969; Lee & Feast 1969). Subsequent studies showed the dust to be at an equivalent blackbody temperature of 500–1000 K and present around almost all R CrB stars (Feast & Glass 1973; Feast et al. 1977; Glass 1978) but not distributed in a spherically homogeneous shell (Forrest, Gillett, & Stein 1972). Later observations, including measurements of optical polarization, suggested that the dust may be ejected in a preferred plane (Stanford et al. 1988; Rao & Raveendran 1993; Clayton et al. 1997). Feast et al. (1977) showed that for RY Sgr, a 38 day pulsating R CrB star, the intensity of the 3.5 μm emission from the warm dust varied with the same period as the visual light, showing that the dust was heated by starlight. This variation was shown to continue with no significant decline in mean intensity when the star experienced a deep visual decline. The mean intensity did, however, drop at times when the star remained at maximum light. This extended series of infrared observations shows that the circumstellar shell is composed of discrete clouds; should a cloud form along the line of sight to the star, a decline is witnessed, but the heating of the collection of clouds that make up the circumstellar shell is little affected because only a modest fraction of the stellar surface is blocked from directly heating the shell. *IRAS* observations revealed, in addition to the warm dust detected from the ground, an extended "fossil" shell of cold ($T \sim 30$ K) dust (Gillett et al. 1986; Rao & Nandy 1986; Walker 1986).

The attribution of emission and absorption features in spectra of circumstellar shells around C-rich objects has been contested. Two leading proposals vie for identification of emission features: polycyclic aromatic hydrocarbons and hydrogenated amorphous carbon. Since R CrB stars are H-deficient to different degrees, observation and analysis of their infrared emission features afford an opportunity to investigate the role of hydrogen in formation of the very large molecules or dust grains. Hydrogen deficiency and other circumstances peculiar to R CrB circumstellar shells may promote the formation of other species.

With the advent of the *Infrared Space Observatory* (*ISO*; Kessler et al. 1996), there came an opportunity to obtain infrared spectra of R CrB stars in and beyond the narrow windows open to ground-based observers. In this paper, we discuss and interpret spectra of three R CrBs obtained with *ISO* over the wavelength region 2.5–45 μm. At the H-rich end of the range is V854 Cen, with an H-abundance that is a factor of only 100 below normal. We contrast V854 Cen with RY Sgr and R CrB, two stars with considerably less hydrogen than V854 Cen.

[1] Based on observations with *ISO*, an ESA project with instruments funded by ESA member states (especially the PI countries: France, Germany, the Netherlands, and the UK) and with the participation of ISAS and NASA.

2. OBSERVATIONS

2.1. *The Stars*

Two stars were satisfactorily observed under our *ISO* program: RY Sgr and V854 Cen. Data for R CrB were retrieved from the *ISO* archive. Details of the observations, including the parameters of Target Dedicated Time (TDT) and Astronomical Observation Template (AOT), are summarized in Table 1. At the time of observation, RY Sgr and R CrB were close to maximum light, according to the light curves of the American Association of Variable Star Observers. When observed, V854 Cen appeared to have been recovering from minimum light; the V magnitude, according to Lawson et al. (1999), was about 7.7, or 0.5 mag below maximum light.

2.2. *Spectra: Reduction and Calibration*

The spectra were obtained with the Short-Wavelength Spectrometer (SWS; de Graauw et al. 1996) on the *ISO* spacecraft. Spectra were recorded on separate 1×12 detector arrays. The complete spectrum was recorded as 12 different but overlapping spectral bands, using different combinations of grating, aperture, and detector array. Our spectra of RY Sgr and V854 Cen were observed at the slowest scanning speed and, therefore, the highest SWS resolving power of $R = \lambda/\Delta\lambda \sim 1000$. The archived R CrB spectrum had been taken at a higher speed and lower resolving power ($R \sim 400$).

Standard pipeline processing of the raw SWS data involves three principal steps: subtraction of the dark current, assignment of the wavelength scale, and determination of the absolute fluxes. Dark current measurements were obtained just prior to and just after an observation. These were averaged and subtracted from the signal from the source. Wavelengths were calculated from the recorded grating positions and grating constants in the SWS database (Valentijn et al. 1996). Similarly, the raw signals were converted to absolute fluxes (in janskys) using calibrations in the SWS database. Each of the 12 bands was reduced separately, and they were then combined to form a composite spectrum.

The output of the pipeline processing was a spectrum with discontinuities across the edges between adjacent bands. Additional reduction procedures were then applied using the interactive software ISAP (Roelfsema et al. 1993). Spectra in the 12 bands were grouped into four larger bands covering the wavelength regions 2.35–4.1, 4.0–12.0, 12.0–28.0, and 29.0–45.2 μm. A spectrum from a single detector was inspected for abrupt jumps in signal level and for excessive noise levels. Detectors so affected were dropped from the sample. A few bad data points were edited out. Following recommendations by R. Loidl (2000, private communication), we reduced the discontinuities by applying additive corrections relative to the signal from a reference detector within each AOT band selected based on two criteria: (1) it should provide the smallest discontinuity at the band edges and a slope that is most consistent with other detectors, and (2) the mean flux level should not be changed by the choice of detector. The first band (2.4–2.6 μm) was taken as the flux reference. We found that band 7 (7–12.0 μm) showed a significant offset between the scanning directions; the "down" scan spectra were always of higher flux than the "up" scan spectra. This was attributed to "memory effects," and the downscans were rejected. This procedure provided spectra of higher signal-to-noise ratio (S/N) than achieved in all of our earlier attempts to eliminate the discontinuities. Final spectra, after rebinning to a resolving power of $R = 1000$ for RY Sgr and V854 Cen and $R = 400$ for R CrB, are shown in Figure 1.

2.3. *Spectral Energy Distributions*

Since the stars are of variable flux in the infrared, we should not expect the *ISO* fluxes to exactly match published fluxes. V854 Cen was caught by *ISO* in an unusually bright phase at infrared wavelengths; for example, the *ISO* flux density at 10 μm is 25 Jy, while *IRAS* found it to be 15 Jy. *IRAS* fluxes for RY Sgr are 60%–70% higher than the *ISO* fluxes. R CrB was about 40% brighter as observed by *ISO* than by *IRAS*. Walker et al. (1996) observed R CrB with *ISO* when the star was at minimum light, i.e., 7 mag below maximum light. The ISOPHOT instrument was used for photometry at six bandpasses from 60 to 200 μm, and a low-resolution spectrum was acquired from 2.5 to 5 μm and from 5.8 to 11.6 μm, at a resolving power of about 100. The *ISO* photometry seems to show that R CrB was a factor of about 2 brighter at minimum than it was when measured with *IRAS*. The 2.5–11.6 μm spectrum differs in shape from ours but does not differ in average flux: the ISOPHOT spectrum shows less flux than the SWS spectrum for wavelengths shorter than about 4 μm and longer than about 8.5 μm, with differences largest at the wavelength limits of the ISOPHOT spectrum. Between 4 and 8.5 μm, the ISOPHOT spectrum has the higher flux by up to about a factor of 2. The ISOPHOT spectrum cannot be fitted well by a blackbody spectrum.

Infrared excesses are conveniently expressed using a fit of a blackbody spectrum after consideration of the photospheric spectrum. This is an adequate artifice here because we are primarily interested in the emission and absorption features. Predicted fluxes from model atmospheres show that the infrared photospheric flux is essentially identical to

TABLE 1

SWS OBSERVATIONS

STAR	DATE[a] UT	JD′	V[b]	TDT	AOT	SPEED
V854 Cen.....	1996 Sep 9	50336	7.7	29701401	SWS01	4
R CrB	1998 Jan 15	50828	6.1	79200268	SWS01	2
RY Sgr	1997 Mar 25	50533	6.6	49500503	SWS01	4

[a] JD = JD′ + 2,400,000.
[b] See text.

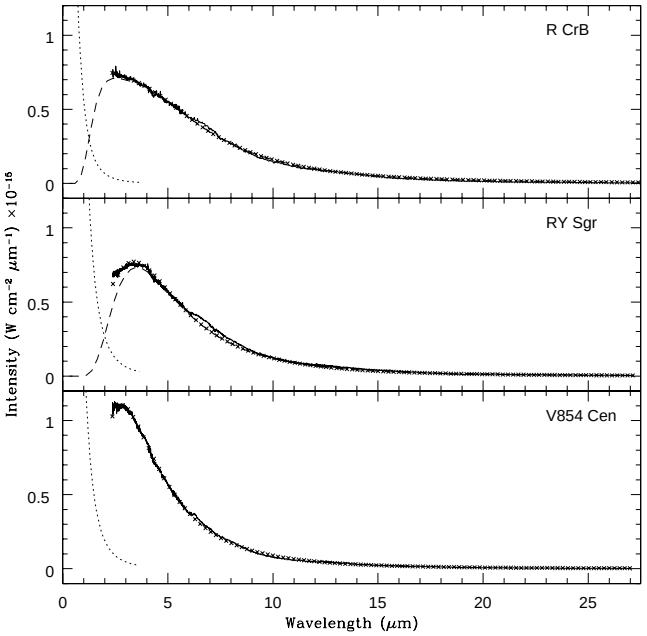

FIG. 1.—*Solid lines*, *ISO* SWS spectra of R CrB, RY Sgr, and V854 Cen; *dotted lines*, adopted photospheric continuum. Assumed effective temperatures are 6900 K (R CrB), 7250 K (RY Sgr), and 6750 K (V854 Cen). *Dashed line*, the blackbody continuum from the circumstellar dust for R CrB and RY Sgr, for the temperatures given in the text; *crosses*, sum of the dust and photospheric continuua. In the case of V854 Cen, the very small contribution of the photospheric continuum is neglected and the crosses give the dust continuum. Excess emission over the fitted fluxes is more clearly displayed in Figs. 2 and 3.

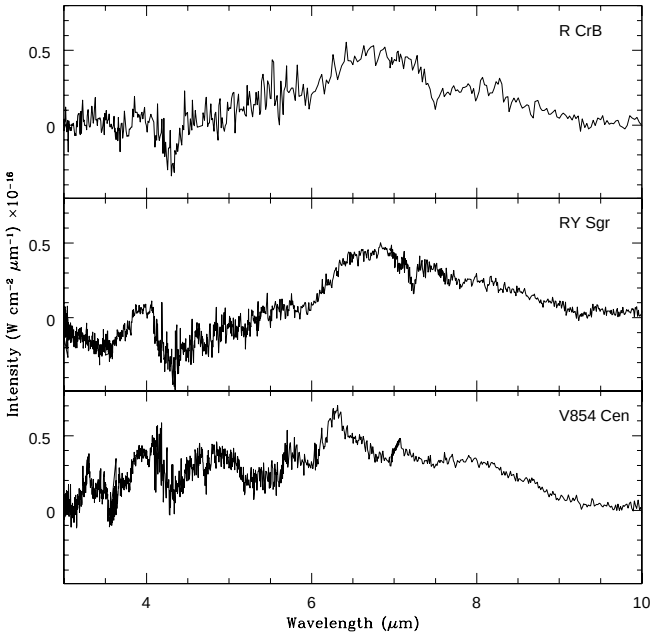

FIG. 2.—Difference spectra of R CrB, RY Sgr, and V854 Cen at 3–10 μm. These are the *ISO* SWS spectra after subtraction of the stellar and circumstellar continua, i.e., solid line of Fig. 1 minus the fitted distribution (*crosses*). Note the change of flux scale.

that of a blackbody at the stellar effective temperature (Asplund et al. 1997a, 1997b). We resolve the observed spectrum into photospheric and circumstellar components; the former does not exceed a 10% contribution at the short-wavelength end of the SWS bandpass. Then, we fitted the circumstellar spectrum with that of a blackbody. Figure 1 shows the photospheric and circumstellar components with the observed spectra. In Figures 2, 3, and 4, the blackbody contribution is subtracted to show more clearly the emission and absorption features that may be present. Over the SWS spectrum, interstellar reddening, slight at B and V, is negligible.

For V854 Cen and RY Sgr, the infrared excess is well fitted by a single blackbody: temperatures of 1040 ± 20 and 820 ± 10 K are obtained for V854 Cen and RY Sgr, respectively. The former temperature is slightly hotter than the 900 K estimated by Lawson & Cottrell (1989) from *IRAS* measurements, but it is equal to the excitation temperature of circumstellar C_2 molecules reported by Rao & Lambert (2000). Our temperature for RY Sgr fits the *IRAS* measurements; Walker (1985) derived a blackbody temperature of 800 ± 50 K from a fit to broadband measurements out to 60 μm. A range of 600–900 K was found by Feast et al. (1977) from ground-based photometry. Fitting the R CrB *ISO* spectrum requires two blackbody components: one at $T = 610 \pm 60$ K provides an adequate fit at wavelengths longer than 5 μm, and a contribution from a hotter blackbody, $T = 1390 \pm 270$ K, is needed to fit the shorter wavelengths. Walker (1985) obtained a temperature of 650 ± 50 K from *IRAS* broadband fluxes from 12 to 100 μm. We note that the *IRAS* observations suggested a similar ($T = 680$ K) dust temperature (Rao & Nandy 1986). In each case, the blackbody simulation of the SWS spectrum fits the observations to a few percent, with small deviations largely arising from emission features.

Our adoption of a blackbody to represent the infrared fluxes is an artifice that enables us to display more clearly the emission features. Representation of an infrared flux distribution by a blackbody is tantamount to assuming that either the dusty clouds are isothermal and optically thick at all wavelengths, or the clouds are optically thin with an absorption coefficient that is quasi-gray in the infrared. An attempt to model the clouds as optically thin was made using laboratory measurements of the nongray absorption coefficient for amorphous carbon samples from Colangeli et al. (1995; see also Bussoletti et al. 1987); the measurements

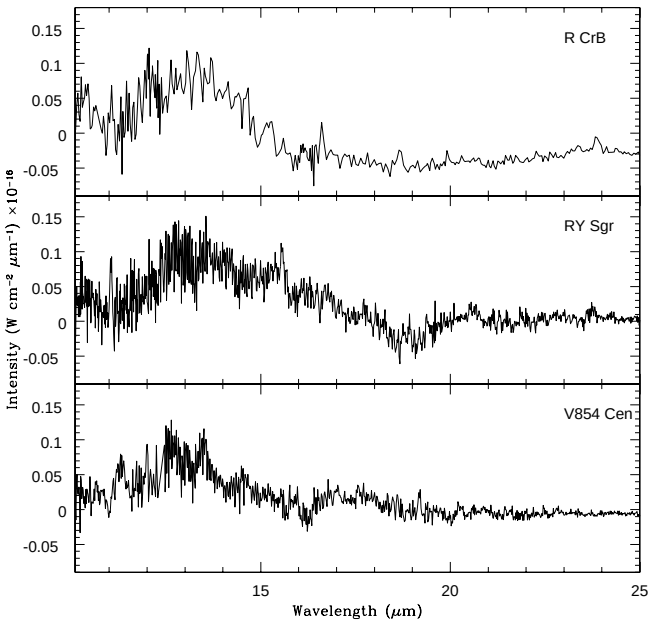

FIG. 3.—Same as Fig. 2, but for 10–25 μm

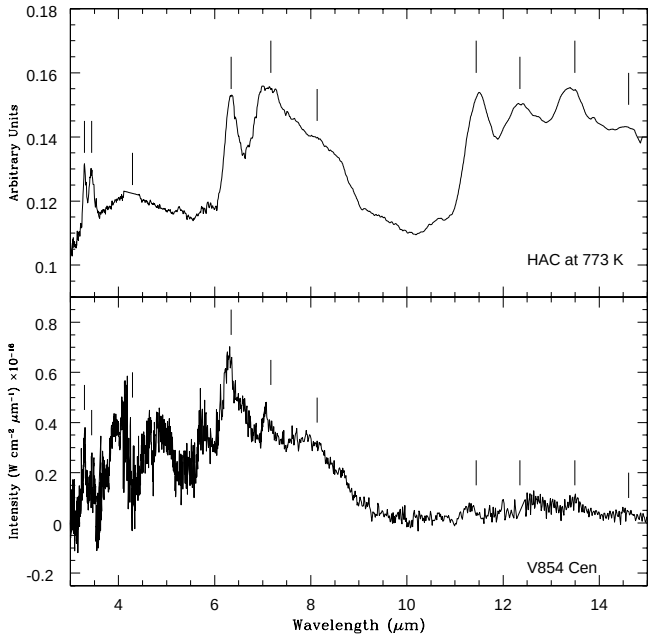

FIG. 4.—Comparison of the difference spectrum of V854 Cen and the laboratory emission spectrum of HAC at 773 K, from Scott, Duley, & Jahani (1997).

for their BE sample were adopted; the BE sample consists of amorphous carbon grains that are produced by burning of benzene in air at normal conditions, using homogenous condensation techniques. The inferred dust temperature is slightly lower, and the overall fit to the observed fluxes is somewhat inferior to the results for the optically thick case. Presumably, the latter result is, in part, due to the failure of the adopted laboratory-measured absorption coefficients to represent the actual circumstellar dust; the laboratory results depend on how the amorphous carbon is prepared. More refined models than either of our simple optically thick and thin approximations would presumably provide higher quality fits, but our present purpose of investigating the narrow emission features is served adequately by adopting the blackbody fit to the spectrum.

Amorphous carbon particles show increased absorption between about 6 and 14 μm (see, e.g., Fig. 5 of Colangeli et al. 1995), which appears to account for the broad emission seen from all three R CrB stars. In the optically thick case, one expects these features to appear in absorption, on the grounds that the temperatures of dust grains on the outer edges of clouds will decrease toward the surface facing away from the star. Optically thin clouds will show emission bands associated with the increased absorption. The measurements by Colangeli et al. and the temperatures found from the optically thin fit to the infrared fluxes provide a rough fit to the broad emission features.

3. EMISSION AND ABSORPTION FEATURES

3.1. *Unidentified Infrared Emissions*

The principal goal of this investigation was to search for spectral features. Such features are seen in the residual or difference spectra (Figs. 2 and 3), obtained by subtracting the best-fitting blackbody spectrum from the observed spectrum. Emission features may be classified as "broad" or "narrow." Narrow features are seen only in V854 Cen, while broad features are seen in all three R CrB stars.

V854 Cen.—The narrow emission features (Table 2) seen in V854 Cen's spectrum correspond to some of the famous unidentified infrared (UIR) features seen in emission from many post–asymptotic giant branch stars, planetary nebulae, and H II regions. The 3.29 μm UIR feature is certainly present (Fig. 2), and the 3.4 μm UIR feature is possibly present, but the UIR feature at 3.51 μm is not seen above the noise. In the 5–10 μm interval, the UIR features at 6.29 μm stand out above the noise and/or the smooth profile of the broad feature that extends from 6 to 9 μm, but those at 5.6, 6.9, 7.3, 7.7, and 8.6 μm do not. Three UIR features are seen in the 10–25 μm region (Fig. 3); emission is clearly seen at 11.3, 13.5, and possibly at 14.6 μm. The latter two UIR features were discovered in the *ISO* spectra of the Red Rectangle (Waters et al. 1998).

The remaining emission features are broad. A feature appears at 3.95 μm, but it occurs at the border of two spectral bands. The 6.3 μm UIR feature appears at the short-wavelength limit of a broad feature extending to about 9 μm, with local peaks at 6.9 μm (possibly the intrusion of the 6.9 μm UIR feature) and 8.1 μm. Clayton et al. (1995) observed V854 Cen at 8.5–8.8 μm, at a resolving power of 1000; they found a featureless continuum, an observation consistent with our spectrum. An apparently broad feature at 12.6 μm is bracketed by UIR features at 11.3 and 13.5 μm. Inspection of Buss et al.'s (1993) collection of 6–13 μm spectra of "transition objects" (i.e., stars evolving from the AGB to the planetary nebula phase) reveals a gross similarity between V854 Cen and the C-rich proto–planetary nebula IRAS 22272+5435. The spectrum of V854 Cen is definitely different from those of the planetary nebulae NGC 7027 and CPD $-56°8032$.

RY Sgr.—Two broad features are present. One extends from about 6 to 9 μm, and the second from about 11 to 18 μm. There is little evidence of structure within these features. Except for the presence of the 6.3 μm feature in V854 Cen, the appearance of these broad features is similar for V854 Cen and RY Sgr. Clayton et al. (1995) obtained a spectrum of the interval 8.2–8.8 μm at a resolution of 1000 and reported that it was featureless, a result consistent with our spectrum. The *IRAS* Low Resolution Spectrometer (LRS) spectra shown by Clayton et al. (1995) provides a marginal detection of the 11.5–15 μm feature and clear evidence for stronger emission extending from the 8 μm limit of the LRS spectrum to 9 μm, which we identify with the 6–9 μm broad emission feature.

R CrB.—Again, two broad emissions are present. We confirm the 6–9 μm feature found by Buss et al. (1993) and partially recorded on the *IRAS* LRS 8–22 μm spectrum (Clayton et al. 1995). An emission peak at 6.5 μm in the

TABLE 2

V854 CENTAURI: NARROW EMISSION FEATURES

λ (μm)	FWHM (μm)	Flux (10^{-17} W cm^{-2})	UIR?[a]
3.294 (02).....	0.052 (02)	0.116 (12)	Yes
6.298 (10).....	0.177 (11)	0.378 (70)	Yes
11.280 (10).....	0.443 (11)	0.363 (30)	Yes
13.490 (17).....	0.220 (20)	0.100 (20)	Yes

NOTE.—Estimated uncertainties are given in parentheses following each entry, e.g., 3.294 (02) = 3.294 ± 0.002.

[a] See list of UIR features at http://www.ipac.caltech.edu/iso/lws/unidentified.html.

feature reported by Buss et al. (1993) is not confirmed. A second broad feature extends from 11.5 to about 15 μm. Both features commence at the same wavelength in all three stars but span a shorter wavelength interval in R CrB than the apparently similar features in V854 Cen and RY Sgr.

Absorption near 4.6 μm seen in V854 Cen and RY Sgr is likely due to the fundamental vibration-rotation absorption lines from circumstellar CO molecules. Absorption at 7.2 μm in RY Sgr appears to be real; the feature is present in each of the scans of this interval.

3.2. *A Search for* C_{60}

Goeres & Sedlmayr (1992) may have been the first to have considered the spherical cage molecule buckminsterfullerene, C_{60}, as a possible constituent of dust clouds around R CrB stars. Their theoretical model predicted low abundances of C_{60} molecules. This prediction could be circumvented if the carbon-rich gas contained H atoms. Formation of large C-containing molecules is facilitated in the presence of H-containing molecules such as acetylene (C_2H_2) and by photoerosion of hydrogenated amorphous carbon. This suggests that the dust clouds of V854 Cen might harbor C_{60} molecules, even if RY Sgr and R CrB do not. Understanding molecule and dust formation in the outer atmosphere of an R CrB (or any!) star is far from complete. Therefore, a search for these very stable carbon cages is of interest.

Laboratory infrared spectroscopy of free C_{60} molecules has shown that the strongest of the 46 possible vibrational bands are at 7.0, 8.4, 17.4, and 18.8 μm (Nemes et al. 1994; see also Krätschmer et al. 1990; Frum et al. 1991). The given wavelengths are laboratory measurements extrapolated to a temperature of 0 K. Positions (and profiles) of these bands will vary with the temperature of the gas as more and more levels of the rotational ladder are populated with increasing temperature. Nemes et al. (1994) estimate, for example, that at 1000 K the 8.4 μm band head will be seen at 8.58 μm, with a width of 0.1 μm. It is possible that some molecules may be ionized—positively or negatively—in the dust clouds. Infrared spectroscopy of C_{60}^+ molecules in a rare gas matrix has provided measurements of vibrational bands of the ion C_{60}^+ at 7.1 and 7.5 μm (Fulara, Jakobi, & Maier 1993); expected bands at longer wavelengths were not investigated. The negative ion C_{60}^- had strong bands at 7.2 and 8.3 μm. These measurements include a matrix-dependent shift, but the bands of the gas-phase ions will be close to the measured positions. Temperature dependence of the band positions and widths will occur, as they do for C_{60}, for the free cations and anions.

Clayton et al. (1995) searched unsuccessfully for the C_{60} 8.6 μm band on ground-based $R = 1000$ spectra of the interval 8.49–8.82 μm at an S/N of about 100 for R CrB but somewhat lower for V854 Cen and RY Sgr; the wavelength of 8.6 μm is that expected for C_{60} absorption at 1000 K. We confirm that the feature is not present (the S/Ns at 8.5 μm are 60 [V854 Cen], 70 [RY Sgr], and 80 [R CrB]). Our SWS spectra permit a search for the other strong bands. A feature appears near the 7.1 μm band in V854 Cen, but this is at the boundary of two SWS bands, and therefore we doubt that it is a real emission feature. This wavelength is also close to that of bands measured for matrix-isolated C_{60}^+ and C_{60}^-. Other bands of these ions at 7.5 μm for C_{60}^+ and 8.3 μm for C_{60}^- are not present in our spectra. At longer wavelengths (Fig. 3), we do not detect the C_{60} 17.5 and 19.0 μm bands. An apparent emission feature at 19.2 μm is an artifact.

3.3. *The* [Ne II] 12.8 μm *Line*

Optical spectra of R CrBs in deep declines show a few broad emission lines with base widths of 400–600 km s^{-1}. Carriers of permitted broad lines include He I, Na I D, Ca II, and the C_2 molecule. Forbidden broad lines of [N II], [O II], and other atoms and ions have been noted. Detailed reports for V854 Cen (Rao & Lambert 1993) and R CrB (Rao et al. 1999) list and discuss the detected lines. Broad lines, if present, would be resolved on the SWS $R = 1000$ spectra. Broad lines, which are detectable only after a star has faded by several magnitudes, are not to be confused with sharp "chromospheric" lines, primarily from neutral and singly ionized metals, seen early in and throughout a decline. Sharp lines would not be resolved on our spectra.

Gas emitting the optical broad forbidden lines should also emit the [Ne II] 12.8 μm line. If the gas is of low electron density, as indicated for V854 Cen by the intensity ratio of the red [S II] lines (Rao & Lambert 1993), the predicted flux of the [Ne II] line is about 0.3% that of the [N II] 6584 Å line for equal abundances of the ions N^+ and Ne^+. Considerations of elemental abundance and rough estimates of the ionization conditions suggest that the predicted flux of the [Ne II] line is several orders of magnitude smaller than the detection limit. Optical [O I] and [C I] lines observed in spectra of R CrB at minimum light indicate electron densities in excess of the critical densities for [N II] and [Ne II] lines. Then, the fluxes in the [N II] and [Ne II] lines are comparable for equal ionic densities, but even in this more optimistic case, the flux of the 12.8 μm line is at least a factor of 100 smaller than the detection limit. We conclude that the absence of the 12.8 μm [Ne II] line is consistent with optical detections of forbidden lines.

4. DISCUSSION

4.1. *Hydrogenated Amorphous Carbon Dust*

Surely the most intriguing result from these *ISO* spectra is the presence of some UIR features in V854 Cen but not in RY Sgr and R CrB. One may suspect this difference is related to the fact that V854 Cen is less H-deficient than the other two stars. Then those UIR features seen in V854 Cen would likely arise from transitions involving H and C bonds in free molecules, large clusters, or grains.

Analyses of the UV extinction by R CrB stars suggested that the dust is amorphous carbon (Hecht et al. 1984). Laboratory studies of absorption and emission infrared spectra of aggregates of submicron particles or thin films of partially hydrogenated amorphous carbon (HAC) have been reported with a view to identifying the UIR features (Borghesi, Bussoletti, & Colangeli 1987; Scott & Duley 1996; Scott, Duley, & Jahani 1997). In many cases, the precise profile of the absorption or emission feature depends on the thermal history of the laboratory sample. Nonetheless, there is a correspondence between the narrow emission features seen in the spectrum of V854 Cen and the laboratory spectra of HAC. This is well illustrated in Figure 4, where the emission spectrum of a thin HAC film at 773 K from Scott et al. (1997) is plotted with our spectrum of V854 Cen. The temperature of 773 K was the highest temperature investigated by Scott et al. A majority of the emission features seen in the laboratory spectrum are identifiable in the

spectrum of V854 Cen; absorption at 4.3 μm in V854 Cen presumably masks the emission seen in the laboratory spectrum at a similar wavelength, and the laboratory emissions at 7.1 and 12.3 μm are not seen as distinct peaks in the stellar spectrum. Apart from differences in the laboratory and stellar profiles of the 7–9 μm and 11–15 μm bands, there is an obvious difference in the relative strengths of these bands: the ratio of the shorter to the longer wavelength emission is much greater for the stellar than for the laboratory spectrum.

In the laboratory experiments, the intensity of the 3.4 μm feature, characteristic of aliphatic hydrocarbons, decreased as the temperature was raised from 425 to 775 K, and the intensity of the 3.29 μm feature, attributable to aromatic hydrocarbon and seen in V854 Cen, appeared and strengthened. This change was attributed by Scott et al. to the transformation of HAC from a polymer to a protographitic solid. In V854 Cen, the dominant emission is at about 3.3 μm rather than 3.4 μm. The 6.2 μm (aromatic C—C ring vibration) and 11.3 μm (aromatic CH bending mode) are also more intense at the higher temperatures. Emission corresponding to the CH bending modes is also apparent at 12.3 and 13.2 μm in the 773 K laboratory spectra and in V854 Cen. In short, these and other comparisons of relative intensities suggest that a laboratory spectrum at a temperature higher than 773 K, perhaps at the temperature of 1040 K of the dust shell, would prove to be an even closer match to the narrow features of V854 Cen. UIR features seen in astronomical sources at 7.7 and 8.6 μm are apparently absent from V854 Cen and were also reported as absent by Borghesi et al. (1987) in their studies of absorption spectra of small HAC grains. The 7.7 μm feature was attributed to a CN stretch of an NH_2 group that, owing to a lack of N in the laboratory samples, did not appear in laboratory spectra. Nitrogen is not especially abundant in V854 Cen, and therefore absence of this 7.7 μm UIR feature is likely and understandable.

RY Sgr and R CrB show broad emission features similar to those seen from V854 Cen, but the sharp features are exclusive to the latter star. Profiles of the 7–9 and 11–15 μm bands differ from star to star. Apart from the sharp features shown by V854 Cen, the spectra of V854 Cen and R CrB are the most similar. The 7–9 μm band appears resolvable into two bands with minimum flux at about 7.4–7.6 μm, and the emission in the longer wavelength band does not extend beyond about 15 μm. By contrast, RY Sgr's 7–9 μm band does not show the minimum, and emission in the longer wavelength band extends to about 18 μm. These broad emission bands would appear to be a property of dehydrogenated amorphous carbon (see Koike, Hasegawa, & Manabe 1980; Bussoletti et al. 1987; Colangeli et al. 1995).

Hydrogenated amorphous carbon accounts well for the narrow emission features of V854 Cen. Absence of strong features at 7.7 and 8.6 μm that are characteristic of polycyclic aromatic hydrocarbons (PAHs) suggest the free molecules are not abundant in its circumstellar shell. Amorphous carbon formed in a hydrogen-containing atmosphere is composed of randomly oriented, linked, and connected PAH clusters, and therefore, the spectrum of HAC will resemble that of free PAHs, with bands blurred, shifted, and blended by solid-state effects. By an extension of this argument, it is not surprising that an overall match to the HAC spectrum is also found from laboratory spectra of coals such as anthracite and semianthracite (Guillois et al. 1996; Papoular et al. 1996). We suppose it more probable that HAC, rather than coal, forms in the circumstellar shell of V854 Cen.

4.2. *Energy Budget*

It is of interest to investigate the energetics of the dust clouds, which we assume are heated solely by the absorption of starlight. Circumstellar dust is distributed in clouds around the star. After full recovery from a decline, a star always returns to the same brightness. Therefore it is plausible to suppose that at these times there is no cloud along the line of sight. Although detailed comparisons are lacking, available comparisons of observed (corrected for interstellar extinction) and predicted stellar flux distributions around visible wavelengths (see Fig. 8 of Asplund et al. 1997a for R CrB) suggest that circumstellar extinction by small particles is not present at maximum light; large particles producing gray extinction cannot be ruled out by this comparison. Gray extinction from a changing cloud of large particles would cause fluctuations in the brightness of a star at maximum light. If large dust particles are made in the cloud responsible for a decline, they cannot persist in the line of sight once spectroscopic manifestations of a decline (i.e., sharp emission lines) have disappeared in the recovery to maximum light.

Given these assumptions, there is a simple inequality that must be satisfied by the integrated infrared emission from the dust (f^d) and the integrated stellar flux (f^*), where f denotes the flux received at the Earth. The inequality is $f^d < f^*$ and reflects the facts that (1) the dust clouds may be optically thin, and (2) the clouds may not subtend 4π of solid angle at the star. The dust emission f^d is estimated as described above from the measured spectrum after subtraction of a small contribution from the star. Stellar emission f^* is estimated from published $UBVRIJ$ magnitudes at maximum light, with estimates added for the ultraviolet flux from IUE spectra and for flux beyond J.

With the ISO fluxes, we find $f^d/f^* \simeq 0.9$ for V854 Cen and 0.4 for R CrB and RY Sgr. The larger ratio for V854 Cen may well result from the fact that we observed the star in the recovery from a deep decline when the infrared fluxes were enhanced owing to a contribution from the recently formed dust cloud that caused the decline. This suggestion is consistent with Forrest's (1974) observations of R CrB showing that the infrared flux increased after mininum light, with f^d/f^* increasing from 0.2 to 0.7 by his estimates. Noting too that the $IRAS$ fluxes for RY Sgr were 60%–70% higher than the ISO fluxes, we suggest $f^d \sim 0.5 f^*$ for these three stars at maximum light between declines. Near-equality of f^d and f^* implies that the ensemble of clouds provides a covering factor approaching 4π and that a majority of the clouds are optically thick or almost so. Given this result, it seems surprising that the stars are visible! Or, to phrase this surprise in another way, are there R CrB stars that have eluded discovery because they are embedded in a very optically thick conglomeration of clouds?

If the dust clouds are optically thin, the mass in amorphous carbon can be estimated readily. If the mean absorption coefficient at 7 μm, the peak of the dust emission, is taken from Colangeli et al. (1995) and the stellar distance is derived from the stellar flux at about 1 μm and an assumed stellar radius of 100 solar radii, the dust masses are 2×10^{-8}, 4×10^{-8}, and 3×10^{-8} $M_\odot$ for V854 Cen, R

CrB, and RY Sgr, respectively. These are probably underestimates by a modest factor. At minimum light, an R CrB star is approximately 7 mag fainter than at maximum light. If the obscuring cloud covers the surface uniformly, an optical depth of about 6 at visual wavelengths exists. Given the approximately inverse wavelength dependence of the dust absorption coefficient, the optical depth of the cloud at 8 μm is about 0.4. This estimate for a fresh cloud is likely an overestimate for the typical cloud in the dust shell.

To build a more complete picture of the clouds, imposition of radiative equilibrium is required. Hartmann & Apruzese (1976) were able to fit Forrest's (1974) infrared photometry for infrared maximum and minimum (both corresponding to visual maximum), with dust distributed out to 300–500 stellar radii. Optical depth at infrared wavelengths for the assumed dust distributions is very small. The dust mass derived, about $5 \times 10^{-7}\ M_{\odot}$, is larger than our estimate, but this is possibly due to differences in the adopted absorption coefficients. A recalculation of model circumstellar shells of HAC grains in radiative equilibrium would be of interest.

5. CONCLUDING REMARKS

Dust in a cloud is reluctant to betray its identity. Yet, the *ISO* 3–25 μm spectra of the ensemble of dust clouds around the stars V854 Cen, R CrB, and RY Sgr offer a few new clues. Sharp emission features coincident with certain of the UIR features are present only in the spectrum of V854 Cen and are a fair replica of emission seen in laboratory spectra of hydrogenated amorphous carbon. These associations are consistent with the fact that V854 Cen, although H-poor relative to normal stars, is H-rich by a factor of 1000 with respect to R CrB and RY Sgr. Spectra of all three stars show a double-peaked broad emission feature between 6 and 14 μm that corresponds to a feature in the extinction curve of amorphous carbon. In summary, amorphous carbon is a major contributor to the infrared emission from R CrB stars, and in the case of V854 Cen, the amorphous carbon is hydrogenated.

We are especially grateful to Rita Loidl for advice on how to reduce the SWS spectra. We thank B. Gustafsson and M. Asplund for their interest in this project, and W. Duley for providing the laboratory spectrum illustrated in Figure 4. The *ISO* Spectral Analysis Package (ISAP) is a joint development by the LWS and SWS Instrument Teams and Data Centers, with CESR, IAS, IPAC, MPE, RAL, and SRO as contributing institutions. This research was supported in part by NASA through grants NAG 5-3348 and CITJ-961543.

REFERENCES

Asplund, M., Gustafsson, B., Kiselman, D., & Eriksson, K. 1997a, A&A, 318, 521
———. 1997b, A&A, 323, 286
Borghesi, A., Bussoletti, E., & Colangeli, L. 1987, ApJ, 314, 422
Buss, R. H., Jr., Tielens, A. G. G. M., Cohen, M., Werner, M. W., Bregman, J. D., & Witteborn, F. C. 1993, ApJ, 415, 250
Bussoletti, E., Colangeli, L., Borghesi, A., & Orofino, V. 1987, A&AS, 70, 257
Clayton, G. C., Bjorkman, K. S., Nordsieck, K. H., Zellner, N. E. B., & Schulte-Ladbeck, R. E. 1997, ApJ, 476, 870
Clayton, G. C., Kelly, D. M., Lacy, J. H., Little-Marenin, I. R., Feldman, P. A., & Bernath, P. F. 1995, AJ, 109, 2096
Colangeli, L., Mennella, V., Palumbo, P., Rotundi, A., & Bussoletti, E. 1995, A&AS, 113, 561
de Graauw, T., et al. 1996, A&A, 315, L49
Feast, M. W., Catchpole, R. M., Lloyd Evans, T., Robertson, B. S. C., Dean, J. F., & Bywater, R. A. 1977, MNRAS, 178, 415
Feast, M. W., & Glass, I. S. 1973, MNRAS, 161, 293
Forrest, W. J. 1974, Ph.D. thesis, Univ. California, San Diego
Forrest, W. J., Gillett, F. C., & Stein, W. A. 1972, ApJ, 178, L129
Frum, C. I., Engleman, R., Jr., Hedderich, H. G., Bernath, P. F., Lamb, L. D., & Huffman, D. R. 1991, Chem. Phys. Lett., 176, 504
Fulara, J., Jakobi, M., & Maier, J. P. 1993, Chem. Phys. Lett., 211, 227
Gillett, F. C., Backman, D. E., Beichman, C., & Neugebauer, G. 1986, ApJ, 310, 842
Glass, I. S. 1978, MNRAS, 185, 23
Goeres, A., & Sedlmayr, E. 1992, A&A, 265, 216
Guillois, O., Nenner, I., Papoular, R., & Reynaud, C. 1996, ApJ, 464, 810
Hartmann, L., & Apruzese, J. P. 1976, ApJ, 203, 610
Hecht, J. H., Holm, A. V., Donn, B., & Wu, C.-C. 1984, ApJ, 280, 228
Kessler, M. F., et al. 1996, A&A, 315, L27
Koike, C., Hasegawa, H., & Manabe, A. 1980, Ap&SS, 67, 495
Krätschmer, W., Lamb, L. D., Fostiropoulos, K., & Huffman, D. R. 1990, Nature, 347, 354
Lawson, W. A., & Cottrell, P. L. 1989, MNRAS, 240, 689
Lawson, W. A., et al. 1999, AJ, 117, 3007
Lee, T. A., & Feast, M. W. 1969, ApJ, 157, L173
Nemes, L., Ram, R. S., Berath, P. S., Tinker, F. A., Zumwalt, M. C., Lamb, L. D., & Huffman, D. R. 1994, Chem. Phys. Lett., 218, 295
O'Keefe, J. A. 1939, ApJ, 90, 240
Papoular, R., Conard, J., Guillois, O., Nenner, I., Reynaud, C., & Rouzaud, J.-N. 1996, A&A, 315, 222
Rao, N. K., & Lambert, D. L. 1993, AJ, 105, 1915
———. 2000, MNRAS, 313, L33
Rao, N. K., & Nandy, K. 1986, MNRAS, 222, 357
Rao, N. K., & Raveendran, A. V. 1993, A&A, 274, 330
Rao, N. K., et al. 1999, MNRAS, 310, 717
Roelfsema, P. R., Kester, D. J. M., Wesselius, P. R., Sym, N., Leech, K., Wieprech, E. 1993, in ASP Conf. Ser. 52, Astronomical Data Analysis Software and Systems II, ed. R. J. Hanisch, R. J. V. Brissenden, & J. Barnes (San Francisco: ASP), 254
Scott, A. D., & Duley, W. W. 1996, ApJ, 472, L123
Scott, A. D., Duley, W. W., & Jahani, H. R. 1997, ApJ, 490, L175
Stanford, S. A., et al. 1988, ApJ, 325, L9
Stein, W. A., Gaustad, J. E., Gillett, F. C., & Knacke, R. F. 1969, ApJ, 155, L3
Valentijn, E. A., et al. 1996, A&A, 315, L60
Walker, H. J. 1985, A&A, 152, 58
———. 1986, in Hydrogen Deficient Stars and Related Objects, ed. K. Hunger, D. Schönberner, & N. K. Rao (Dordrecht: Reidel), 407
Walker, H. J., Heinrichsen, I., Richards, P. J., Klaas, U., & Rasmussen, I. L. 1996, A&A, 315, L249
Waters, L. B. F. M., et al. 1998, Nature, 391, 868